Suppressed ionic effect and low-frequency texture transitions in a cholesteric liquid crystal doped with graphene nanoplatelets

Po-Chang Wu,[1] Longin N. Lisetski,[2] and Wei Lee[1,*]

[1]*Institute of Imaging and Biomedical Photonics, College of Photonics, National Chiao Tung University, Guiren Dist., Tainan 71150, Taiwan*

[2]*Institute for Scintillation Materials of STC "Institute for Single Crystals", National Academy of Sciences of Ukraine, Kharkiv 61001, Ukraine*

[*]*wlee@nctu.edu.tw*

Abstract: We focus on investigating the dielectric behaviors and the low-frequency texture transitions in a cholesteric liquid crystal (CLC) doped with graphene nanoplatelets (GNPs) by means of dielectric spectroscopy and measurements of electro-optical responses. The experimental results indicate that incorporating GNPs at a content of 0.5 wt% into the CLC leads to significant suppression of ionic behaviors, as manifested by the reduction in ionic density, diffusivity, and relaxation frequency. In addition, the electro-optical properties of the GNP-doped CLC cell show the lowered operation voltage for the switching from the planar to focal conic state and the absence of the low-frequency focal-conic-to-uniform-lying-helix texture transition. Such results are attributable to the effects of GNPs as nuclei in the CLC medium, giving rise to the repression of the ionic and electrohydrodynamic effects.

OCIS codes: (160.3710) Liquid crystals; (160.1585) Chiral media; (160.4890) Organic materials; (230.3720) Liquid-crystal devices.

References and links

1. D. Berreman and T. Scheffer, "Bragg reflection of light from single-domain cholesteric liquid-crystal films," Phys. Rev. Lett. **25**(9), 577–581 (1970).
2. D.-K. Yang, J. L. West, L.-C. Chien, and J. W. Doane, "Control of reflectivity and bistability in displays using cholesteric liquid crystals," J. Appl. Phys. **76**(2), 1331–1333 (1994).
3. I. P. Ilchishyn, L. N. Lisetski, and T. V. Mykytiuk, "Reversible phototuning of laser frequency in dye-doped cholesteric liquid crystal," Opt. Mater. Express **1**(8), 1484–1493 (2011).
4. M. Xu and D.-K. Yang, "Dual frequency cholesteric light shutters," Appl. Phys. Lett. **70**(6), 720–722 (1997).
5. Y.-C. Hsiao, C.-Y. Tang, and W. Lee, "Fast-switching bistable cholesteric intensity modulator," Opt. Express **19**(10), 9744–9749 (2011).
6. J. Hwang, M. H. Song, B. Park, S. Nishimura, T. Toyooka, J. W. Wu, Y. Takanishi, K. Ishikawa, and H. Takezoe, "Electro-tunable optical diode based on photonic bandgap liquid-crystal heterojunctions," Nat. Mater. **4**(5), 383–387 (2005).
7. O. Stamatoiu, J. Mirzaei, X. Feng, and T. Hegmann, "Nanoparticles in liquid crystals and liquid crystalline nanoparticles," in *Liquid Crystals: Topics in Current Chemistry*, edited by Carsten Tschierske (Springer-Verlag Berlin Heidelberg, 2012) Vol. 318, pp 331–393.
8. W. Lee, C.-Y. Wang, and Y.-C. Shih, "Effects of carbon nanosolids on the electro-optical properties of a twisted nematic liquid-crystal host," Appl. Phys. Lett. **85**(4), 513–515 (2004).
9. B.-R. Jian, C.-Y. Tang, and W. Lee, "Temperature-dependent electrical properties of dilute suspensions of carbon nanotubes in nematic liquid crystals," Carbon **49**(3), 910–914 (2011).
10. C.-W. Lee and W.-P. Shih, "Quantification of ion trapping effect of carbon nanomaterials in liquid crystals," Mater. Lett. **64**(3), 466–468 (2010).
11. H.-H. Liu and W. Lee, "Time-varying ionic properties of a liquid-crystal cell," Appl. Phys. Lett. **97**(2), 023510 (2010).
12. T. Joshi, J. Prakash, A. Kumar, J. Gangwar, A. K. Srivastava, S. Singh, and A. M. Biradar, "Alumina nanoparticles find an application to reduce the ionic effects of ferroelectric liquid crystal," J. Phys. D Appl. Phys. **44**(31), 315404 (2011).
13. C.-Y. Tang, S.-M. Huang, and W. Lee, "Electrical properties of nematic liquid crystals doped with anatase TiO_2 nanoparticles," J. Phys. D Appl. Phys. **44**(35), 355102 (2011).

#234759 - $15.00 USD Received 17 Feb 2015; revised 16 Apr 2015; accepted 16 Apr 2015; published 21 Apr 2015

14. S.-W. Liao, C.-T. Hsieh, C.-C. Kuo, and C.-Y. Huang, "Voltage-assisted ion reduction in liquid crystal-silica nanoparticle dispersions," Appl. Phys. Lett. **101**(16), 161906 (2012).
15. A. Chandran, J. Prakash, P. Ganguly, and A. M. Biradar, "Zirconia nanoparticles/ferroelectric liquid crystal composites for ionic impurity-free memory applications," RSC Adv. **3**(38), 17166–17173 (2013).
16. R. Basu and A. Garvey, "Effects of ferroelectric nanoparticles on ion transport in a liquid crystal," Appl. Phys. Lett. **105**(15), 151905 (2014).
17. O. Kurochkin, O. Buchnev, A. Iljin, S. K. Park, S. B. Kwon, O. Grabar, and Yu. Reznikov, "A colloid of ferroelectric nanoparticles in a cholesteric liquid crystal," J. Opt. A, Pure Appl. Opt. **11**(2), 024003 (2009).
18. A. L. Rodarte, C. Gray, L. S. Hirst, and S. Ghosh, "Spectral and polarization modulation of quantum dot emission in a one-dimensional liquid crystal photonic cavity," Phys. Rev. B **85**(3), 035430 (2012).
19. A. M. Chepikov, S. S. Minenko, L. N. Lisetski, N. I. Lebovka, N. V. Usol'tseva, and M. S. Soskin, "Dispersions of carbon nanotubes and organomodified clay platelets in cholesteric liquid crystals," Funct. Mater. **19**, 343–347 (2012).
20. S.-C. Jeng, S.-J. Hwang, Y.-H. Hung, and S.-C. Chen, "Cholesteric liquid crystal devices with nanoparticle aggregation," Opt. Express **18**(21), 22572–22577 (2010).
21. M. Infusino, A. De Luca, F. Ciuchi, A. Ionescu, N. Scaramuzza, and G. Strangi, "Optical and electrical characterization of a gold nanoparticle dispersion in a chiral liquid crystal matrix," J. Mater. Sci. **49**(4), 1805–1811 (2014).
22. O. Yaroshchuk, S. Tomylko, I. Gvozdovskyy, and R. Yamaguchi, "Cholesteric liquid crystal-carbon nanotube composites with photo-settable reversible and memory electro-optic modes," Appl. Opt. **52**(22), E53–E59 (2013).
23. C.-K. Chang, S.-W. Chiu, H.-L. Kuo, and K.-T. Tang, "Cholesteric liquid crystal-carbon nanotube hybrid architectures for gas detection," Appl. Phys. Lett. **100**(4), 043501 (2012).
24. P.-C. Wu and W. Lee, "Phase and dielectric behaviors of a polymorphic liquid crystal doped with graphene nanoplatelets," Appl. Phys. Lett. **102**(16), 162904 (2013).
25. A. Malik, A. Choudhary, P. Silotia, A. M. Biradar, V. K. Singh, and N. Kumar, "Effect of graphene oxide nanomaterial in electroclinic liquid crystals," J. Appl. Phys. **108**(12), 124110 (2010).
26. C. W. Twombly, J. S. Evans, and I. I. Smalyukh, "Optical manipulation of self-aligned graphene flakes in liquid crystals," Opt. Express **21**(1), 1324–1334 (2013).
27. M. Lavrič, V. Tzitzios, S. Kralj, G. Cordoyiannis, I. Lelidis, G. Nounesis, V. Georgakilas, H. Amenitsch, A. Zidanšek, and Z. Kutnjak, "The effect of graphene on liquid-crystalline blue phases," Appl. Phys. Lett. **103**(14), 143116 (2013).
28. S. Ni, H. Li, S. Li, J. Zhu, J. Tan, X. Sun, C. P. Chen, G. He, D. Wu, K.-C. Lee, C.-C. Lo, A. Lien, J. Lu, and Y. Su, "Low-voltage blue-phase liquid crystals with polyaniline-functionalized graphene nanosheets," J. Mater. Chem. C **2**(9), 1730–1735 (2014).
29. R. Basu, "Effects of graphene on electro-optic switching and spontaneous polarization of a ferroelectric liquid crystal," Appl. Phys. Lett. **105**(11), 112905 (2014).
30. W. Helfrich, "Electrohydrodynamic and dielectric instabilities of cholesteric liquid crystals," J. Chem. Phys. **55**(2), 839–842 (1971).
31. F. Rondelez, H. Arnould, and C. J. Gerritsma, "Electrohydrodynamic effects in cholesteric liquid crystals under ac electric fields," Phys. Rev. Lett. **28**(12), 735–737 (1972).
32. Merck datasheets.
33. Y.-J. Liu, P.-C. Wu, and W. Lee, "Spectral variations in selective reflection in cholesteric liquid crystals containing opposite-handed chiral dopants," Mol. Cryst. Liq. Cryst. (Phila. Pa.) **596**(1), 37–44 (2014).
34. N. I. Lebovka, L. N. Lisetski, M. I. Nesterenko, V. D. Panikarskaya, N. A. Kasian, S. S. Minenko, and M. S. Soskin, "Anomalous selective reflection in cholesteryl oleyl carbonate–nematic 5CB mixtures and effects of their doping by single-walled carbon nanotubes," Liq. Cryst. **40**(7), 968–975 (2013).
35. A. Kumar, P. Silotia, and A. M. Biradar, "Effect of polymeric nanoparticles on dielectric and electro-optical properties of ferroelectric liquid crystals," J. Appl. Phys. **108**(2), 024107 (2010).
36. G. Barbero and A. L. Alexe-Ionescu, "Role of the diffuse layer of the ionic charge on the impedance spectroscopy of a cell of liquid," Liq. Cryst. **32**(7), 943–949 (2005).
37. C.-T. Wang, W.-Y. Wang, and T.-H. Lin, "A stable and switchable uniform lying helix structure in cholesteric liquid crystals," Appl. Phys. Lett. **99**(4), 041108 (2011).
38. Orsay Liquid Crystal Group, "Hydrodynamic instabilities in nematic liquids under ac electric fields," Phys. Rev. Lett. **25**(24), 1642–1643 (1970).

1. Introduction

Liquid crystals (LCs), known for their uniquely anisotropic material properties, have found a wide spectrum of applications in electro-optical and photonic devices, especially the flat-panel displays. Among currently available LC materials, cholesteric LCs (CLCs) are characterized by nematic-like orientational ordering with a helical structure and can be regarded as one-dimensional photonic crystals. The main optical property of a CLC is the presence of a reflection band characterized by the helical pitch and the refractive index which enables the selective reflection at specific wavelengths [1]. When applying voltages to the CLC, two typically stable states—the planar (P) and focal conic states (FC)—can be

#234759 - $15.00 USD Received 17 Feb 2015; revised 16 Apr 2015; accepted 16 Apr 2015; published 21 Apr 2015

achieved. Based on such unique features, CLCs have widely been proposed for applications in memory-enabling reflective LC displays [2], lasers [3] and some other photonic devices such as optical switches, modulators as well as diodes [4–6].

With the aim at further innovation of LC-based devices, incorporation of nanoparticles (NPs) as the dopant in LCs have been extensively considered as a way of non-synthetic approaches for improvement of physical and electro-optical properties of LCs [7]. Moreover, since the presence of ion impurities, originating from the LC substances, alignment layers and electrode materials, can hardly be eliminated, specific types of nanomaterials, such as carbon-based allotropes [8-10], clay platelets [11], alumina (Al_2O_3) [12], anatase (TiO_2) [13], silica (SiO_2) [14], zirconia (ZrO_2) [15] and ferroelectric NPs [16], were introduced as dopants to LC hosts for the purpose of trapping ion impurities and, in turn, recovering the electrical properties of the LCs degraded by the ionic effect. Among recent developments of the nanomaterials dispersion in CLCs, fascinating features, such as the reduction of the operation voltage by the ferroelectric NPs [17], variation of spectral properties by quantum dots [18], carbon nanotubes and clay platelets [19] as well as texture stabilization by polyhedral oligomeric silsesquioxane (POSS) [20] or gold NPs [21], have been reported. In addition, practical applications for gas detection and dual-mode optical devices have also been suggested on the basis of the CLC colloids doped with carbon nanotubes [22,23]. While the ionic effect suppression by the nanodopants have extensively been studied for nematic and ferroelectric LCs, only few works on the ionic behaviors in the nanomaterial/CLC suspensions have been reported [21].

In our previous study, we have investigated ionic and phase behaviors in a colloidal structure with graphene nanoplatelets (GNPs) as a dopant dispersed in the polymorphic LC 8OCB. Key findings concerning the dopant effects include the observations of new crystalline phases, increase in the SmA-to-nematic and nematic-to-isotropic phase transition temperatures due to enhancement of LC ordering, and suppression of the ionic effect by the ion trapping [24]. Other studies of graphene-doped LC systems have shown the controlled alignment in electroclinic LCs [25], controlled optical properties in nematic LCs [26], stabilization of the LC state and improved operating voltage in blue phases [27,28], and enhanced electro-optical switching in ferroelectric LCs [29]. In this work, we consider a colloidal structure of CLC with GNPs dispersed therein, with main attention to the dielectric behavior and electro-optical responses of the hybrid LC material by means of temperature-dependent dielectric spectroscopy and the measurement of voltage-dependent transmission. We firstly present spectral properties of undoped and GNP-doped LC cells, followed by the discussion of the dopant effects of GNPs on ionic behaviors, including the relaxation frequency, ionic density and diffusivity in the CLC. Specifically, since the space-charge energy plays a crucial role in the induction of the low-frequency electrohydrodynamic (EHD) effect in the CLC [30,31], the electro-optical responses of both the GNP-doped and pure CLC cells are compared to clarify the operation voltage and field-induced texture transition behaviors, especially for cells driven by low-frequency voltages.

2. Experiment

The CLC used was composed of the nematic LC E7 doped with the right-handed chiral agent R5011 at concentration of 2.6 wt%. The value of helical twisting power (HTP) of R5011 in E7 is 116 μm^{-1} and the refractive indices of E7 are n_e = 1.7472 and n_o = 1.5217 at the wavelength of 589 nm and temperature of 20 °C [32]. Consequently, the helical pitch p and the central wavelength of the selective reflection, λ_c, of the CLC are calculated as ~336 nm and 550 nm, respectively. As in our previous work [24], we used GNPs produced by XG Science (xGNP-05, ~16 graphene layers with an average thickness of 10 nm and a diameter of 5 μm). The GNPs were dispersed in the CLC at concentration of 0.5 wt%. It is worth mentioning that pretreatment of GNPs was performed, including baking in a vacuum oven to evaporate residual moistures and mechanical ball-milling to prevent the carbonaceous nanoplatelets from aggregation [9]. To promote homogeneity and obtain a uniform dispersion, the CLC–GNP colloid was homogenized in an ultrasonic water bath for 1 h. The

#234759 - $15.00 USD Received 17 Feb 2015; revised 16 Apr 2015; accepted 16 Apr 2015; published 21 Apr 2015

GNP-doped CLC and the neat CLC were individually injected into anti-parallel planar-aligned cells (Mesostate Co.) by capillary action at 65 °C. Each cell had a thickness of 6 ± 0.5 μm and an effective electrode area of 1 cm^2. In this study, the cell temperature within ± 0.1 °C was controlled by a temperature controller ((Linkam T95-PE) in all of the measurements. The optical properties of the samples were studied using a high-speed fiber-optic spectrometer (Ocean Optics HR2000 +) in conjunction with a halogen light source (Ocean Optics HL2000). For the dielectric investigations, the complex dielectric spectra in the frequency range between 1 and 10^5 Hz were acquired with a high-precision LCR meter (HIOKI 3522-50). The probing voltage was 0.1 V_{rms} in the sinusoidal waveform, which was much smaller than the Fréedericksz-transition voltage of the CLC. The electro-optical responses of the cells were considered on the basis of the voltage-dependent transmittance (*V–T%*) curves and observations of optical microscopic images (Olympus BX51). All *V–T%* curves were measured using a He–Ne laser with emission wavelength of 632.8 nm (JDSU 1125), an arbitrary function generator (Tektronix AFG-3022B), and an amplifier (TREK Model 603). Voltage pulses were applied in square waveform at a given frequency. Note that none of any polarizer was employed in this study, except for the observation of optical textures. To ascertain that the measurements were taken in the CLC phase, the phase sequences of the samples were identified by means of the dielectric method [24]. From the first derivative of the real-part permittivity at 10 kHz with respect to the temperature, the values of the CLC-to-isotropic phase transition temperature were determined as 57 °C for the pure CLC and 59 °C for the GNP-doped CLC. The slight increase in CLC-to-isotropic phase transition temperature in the GNP-doped sample results most probably from the enhancement of LC ordering by the GNPs, which was also found in a previous work concerning 8OCB–GNP colloids [24]. As a result, all the measurements were carried out within a temperature range between 21 and 54 °C where the investigated cells were surely in the CLC phase.

3. Results and discussion

Figure 1(a) exemplarily shows that both the selective reflection band and the corresponding optical image of a GNP-doped CLC cell are essentially similar to those of an undoped counterpart at a given temperature *T*. Plotting the central wavelength and the bandwidth $\Delta\lambda$ values at various temperatures using the data of the obtained reflection bands, one can see that

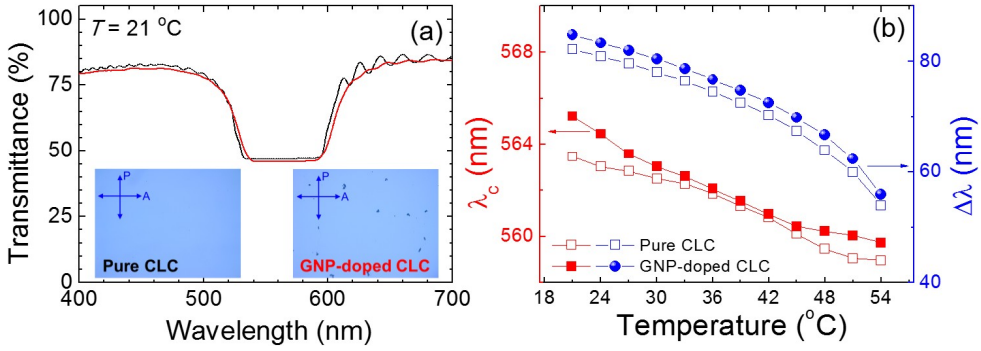

Fig. 1. (a) Transmittance spectra of a pristine cell (back curve) and a GNP-doped CLC cell (red curve) in the unperturbed P state. (b) Calculated central wavelength and bandwidth.

#234759 - $15.00 USD Received 17 Feb 2015; revised 16 Apr 2015; accepted 16 Apr 2015; published 21 Apr 2015

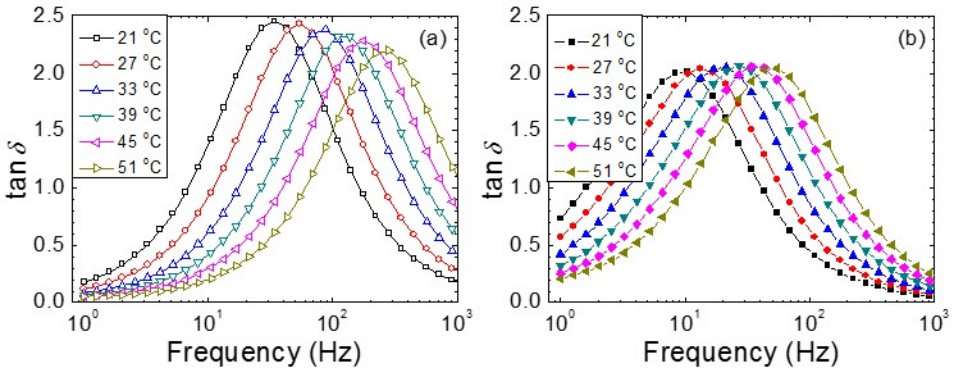

Fig. 2. tan δ spectra of (a) pure and (b) GNP-doped CLCs at various temperatures.

the differences between the doped CLC and the pure one within a designated temperature regime are rather small (Fig. 1(b)). This suggests that GNPs as the dopant dispersed in the CLC do not show a significant effect on the helical structure and thus the optical profile of the Bragg reflection band of the CLC. Note that the slight blueshift of λ_c and decrease in $\Delta\lambda$ with increasing temperature could be probably attributed to the decrease in average refractive index and optical anisotropy of the host LC since the HTP of R5011 has been found to be independent of the temperature in the range studied [33]. Previous experiments carried out within the same ideology for CLC dispersions also showed only very small variations in selective reflection characteristics upon introduction of single-walled carbon nanotubes in CLC at similar concentrations [34].

Figure 2 depicts the loss-tangent (tan δ) spectra at various temperatures of both the neat and doped CLC cells in the frequency (f) range between 1 and 1000 Hz. The electric loss tangent as a dissipation factor of electromagnetic energy is defined by tan $\delta = \varepsilon''/\varepsilon'$, where ε' is the real part and ε'' the imaginary part of the complex dielectric permittivity related to the energy-storage and dissipation within the dielectric medium, respectively. The obtained tan $\delta(f)$ curves reflect the relaxation behavior of the electrode polarization resulting from the migration of mobile ions in response to the ac electric field. Consequently, the shift of the curve towards higher frequencies with increasing temperature for both the undoped and doped CLC cells can be attributable to the promotion of the ion transport at higher temperatures or to an increase in the number of charge carriers contributing to electric conduction in the cells. It is clear from the comparison between Figs. 2(a) and 2(b) that the maximum of tan δ in the GNP-doped cell at a given temperature is lower than that of the pure counterpart, presumably due to the trapping of impurity ions by dispersed GNPs [35]. Moreover, the relaxation frequency f_R, generally determined as the frequency corresponding to the tan δ maximum, is also helpful to characterize the relaxation time of the electrode polarization. Obtaining the f_R values by nonlinearly fitting the data from Figs. 2(a) and 2(b), one can see that f_R varies from 33.9 to 318.4 Hz for the pure CLC and from 10.4 to 54.8 Hz for the doped one when T increases from 21 to 54 °C (Fig. 3). Following the Arrhenius equation [13], here the behavior of $f_R(T)$ is understandable in terms of variation of diffusivity with temperature. Note that the value of f_R in the GNP-doped CLC for each temperature is about five times lower than in the pure CLC. Since the relaxation time, representing the sum of charge and discharge times of ions, is inversely proportional to f_R, it can be implied that the GNPs remarkably decelerate the ion transport in the CLC suspension. When the frequency of applied voltage is lower than f_R, a large quantity of ions will acquire more time to build up the electric double layer at the electrode, leading to the weakening of the effective electric field across the cell thickness. This means that the GNP-doped cell has wider tolerance for the applied frequency with respect to the above-mentioned accumulations of ions near the substrate surfaces.

#234759 - $15.00 USD Received 17 Feb 2015; revised 16 Apr 2015; accepted 16 Apr 2015; published 21 Apr 2015

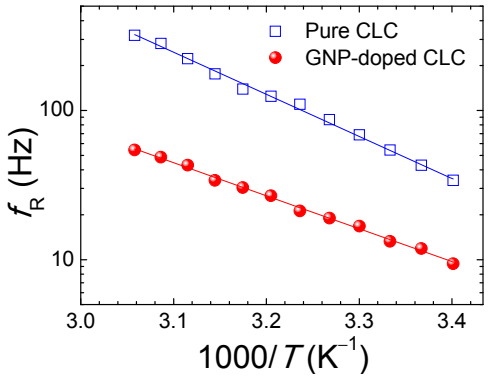

Fig. 3. Relaxation frequency f_R as a function of the absolute temperature T.

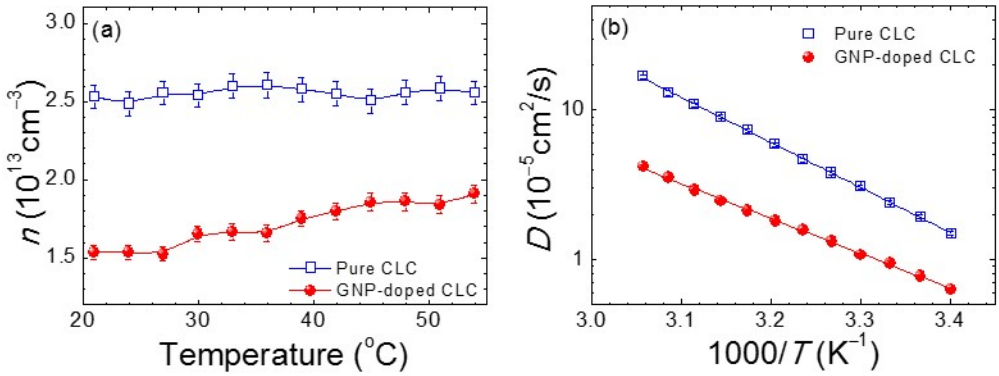

Fig. 4. Deduced (a) ion density n and (b) diffusivity D in undoped and GNP-doped CLC cells.

To quantitatively discuss the influence of GNPs on the ionic behavior of the CLC, Fig. 4 displays the density n and diffusivity D of ions in both samples. Both n and D were deduced by fitting the experimental data of $\varepsilon'(f)$ and $\varepsilon''(f)$ in appropriate frequency ranges according to the following equations [36]:

$$\varepsilon' = \frac{nq^2 D^{3/2}}{\pi^{3/2}\varepsilon_0 d k_B T} f^{-3/2} + \varepsilon_b' \tag{1}$$

and

$$\varepsilon' = \frac{nq^2 D}{\pi\varepsilon_0 k_B T} f^{-1}. \tag{2}$$

Here, q is the electric charge, d is the cell gap, ε_0 is the permittivity in free space, k_B is the Boltzmann constant, T is the absolute temperature, and ε_b' is the intrinsic dielectric constant of the LC bulk. As shown in Fig. 4(a), the value of n, approximately equal to 2.53×10^{13} cm^{-3}, for the pure CLC cell is nearly temperature-independent. This finding is consistent with the behavior observed for the nematic LC E7 [9]. Because the cholesteric helix of the investigated pristine CLC shows weak dependence on temperature [33], the behavior of $n(T)$ for the pure CLC is not due to structural changes but most probably reflects the absence of the ionic association–dissociation reaction [9]. Markedly, the value of n in the GNP-doped CLC is lower as compared with that of the pure counterpart at a fixed temperature. This result arises unambiguously from the trapping of mobile ions by the GNPs since the GNPs do not modify the helical structure of the CLC. The slight increase in n with rising temperature for

#234759 - $15.00 USD Received 17 Feb 2015; revised 16 Apr 2015; accepted 16 Apr 2015; published 21 Apr 2015

the GNP-doped CLC implies weakened ion-trapping efficiency of GNPs at evaluated temperatures. As a result, doping CLC with GNPs at a content of 0.5 wt% decreases the value of n from 2.53×10^{13} to 1.72×10^{13} cm^{-3} in average, yielding a ~32% reduction in n. On the other hand, Fig. 4(b) shows the temperature dependence of diffusivity for both the GNP-doped and pure CLC cells. It is obvious from Fig. 4(b) that the diffusivity of ions in the doped cell is smaller within the whole temperature range studied, suggesting that the GNPs are responsible for restraining the migration of ions in the CLC cell. Since $D(T)$ is related to the viscosity of the CLC and thus to the kinetic energy of ions, the decrease in D in the GNP-doped cell is associated with the enhanced molecular ordering and conglomeration of GNPs, which brings about the increase in viscosity of the LC colloid.

With further discussing the electro-optical responses of the two samples, Fig. 5 shows the V–T% curves of the GNP-doped and pure CLC cells at a fixed temperature of 30 °C. Here, each voltage range where the variation of transmission remains essentially unchanged can be considered as corresponding to a specific CLC state. In the case of f = 1 kHz, the V–T% curves of both cells, as displayed in Fig. 5(a), exhibit two voltage ranges both showing high transmission, separated by an interval with lowered transmission. This means that the behaviors of field-induced texture transition in the GNP-doped and pure CLC are similar. In general, the CLC texture of a cell driven by such a high-frequency (i.e., f = 1 kHz) voltage would sequentially change from the initial P through the FC to the homeotropic (H) state with increasing voltage. Because the wavelength of the laser beam is outside the reflection band of the CLC, both the P and H states are transparent while the FC state is light-scattering state. Moreover, it can be seen from Fig. 5(a) that, as compared to the pure CLC, the voltage for the P-to-FC texture transition ($V_{P–FC}$) decreases from 11 to 6 V in the doped cell. When observing the P-to-FC texture transition in the GNP-doped cell under applied voltages, we noted the formation of FC domains which originate from the GNPs and then expand throughout the cell. Accounting for the anchoring force between GNPs and LC molecules, it is suggested that the GNPs dispersed in the CLC would lead to spatial variations in molecular ordering especially for the molecules in close vicinities of the GNPs. As such, the GNPs can be regarded as defect points for the P-to-FC texture transition. Consequently, the integrity of adjacent helices and the topological equilibrium are more easily destructed in the GNP-doped CLC cell by a lowered voltage.

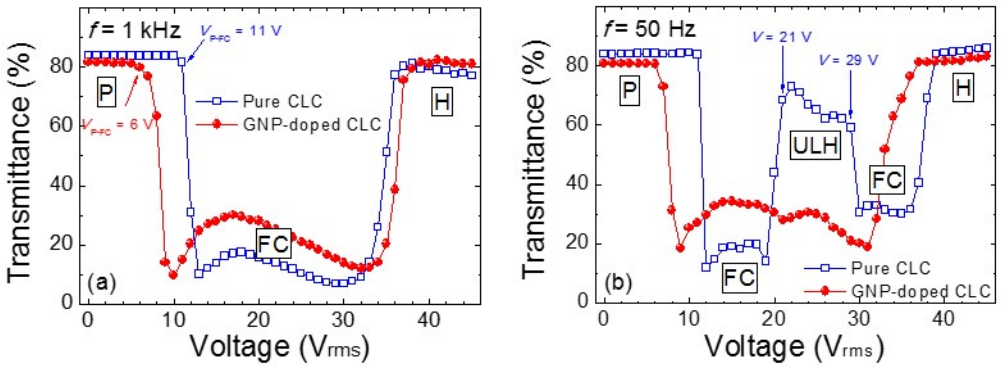

Fig. 5. Voltage-dependent transmittance curves of the GNP-doped and pure CLC cells driven by voltages at frequencies of (a) f = 1 kHz and (b) f = 50 Hz. The data were acquired at T = 30 °C.

#234759 - $15.00 USD Received 17 Feb 2015; revised 16 Apr 2015; accepted 16 Apr 2015; published 21 Apr 2015

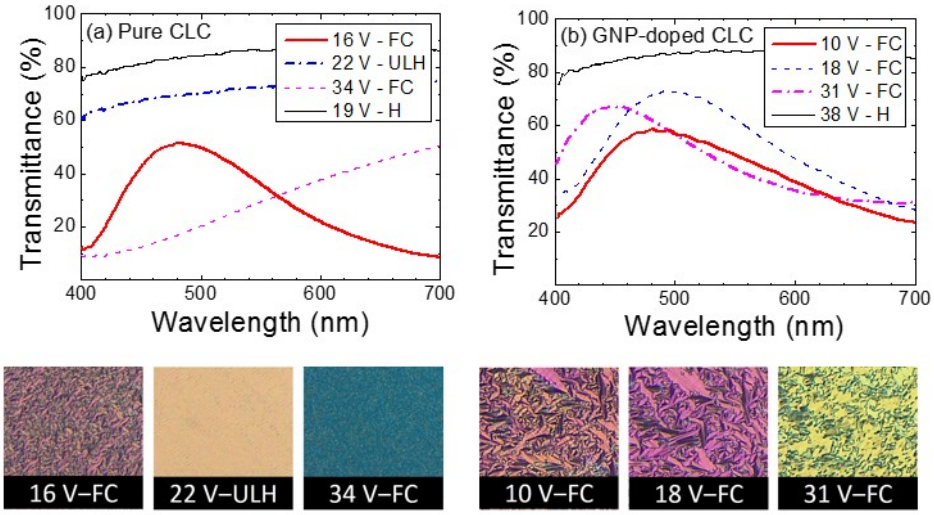

Fig. 6. Transmission spectra and optical images of (a) an undoped cell and (b) a GNP-doped CLC cell driven by designated voltages at frequency of 50 Hz.

Interestingly, as the frequency of applied voltage decreases to, say, 50 Hz, an additional field-induced CLC texture is observed in the voltage regime between 21 and 29 V for the pure CLC cell whereas the texture transition with increasing voltage in the doped CLC cell remains unchanged (Fig. 5(b)). From the transmission spectra and optical textures of each cell under application of specific voltages at f = 50 Hz, it can be concluded that the additional CLC state in the pure CLC cell is the uniform lying helix (ULH) state and the two adjacent states are the FC states with different domain sizes as shown in Fig. 6(a). In considering the low-frequency electro-optical response of the pure E7 cell with planar alignment, we have examined and thus confirmed that the change in transmission with increasing voltage in the frequency regime between 10 and 500 Hz reflects the typical field-induced Fréedericksz transition of LC molecules from the planar to homeotropic alignment and is independent of the applied frequency. Therefore, the field-induced FC-to-ULH texture transition at low frequencies in the CLC cell is unique, presumably due to the ionic agitation and EHD effect in the CLC rather than the induction by the low-frequency response of the LC host E7 [37]. It should be noted that the ULH state is also a transparent state with the helical axis uniformly oriented in parallel to the substrate plane. Because of the molecular agitation by the low-frequency voltage, the transmission in the voltage-sustained ULH state shown in both Figs. 5(b) and 6(a) is lower than that in the H state. Note that the "hump" on the voltage-dependent transmission spectra in the FC states is presumably due to the formation of FC domains of certain sizes weakening the strength of scattering for specific wavelengths. On the other hand, it is confirmed from Fig. 6(b) that the GNP-doped CLC cell in the regime between 10 and 31 V is preserved in the FC state. The difference in the transmission spectra of the GNP-doped cell driven by distinct voltages results from the change in size of the FC domains with varying voltage. Since the low-frequency texture deformation induced by the EHD effect in the CLC cell is dominated by the space charge, it is reasonable to conclude that the absence of the FC-to-ULH state transition in the GNP-doped CLC cell is the result of significant suppression of ionic behavior by the dispersed GNPs. Also, the eventual low-frequency texture deformation can be hindered by the anchoring force of the GNPs to the surrounding LC molecules.

#234759 - $15.00 USD Received 17 Feb 2015; revised 16 Apr 2015; accepted 16 Apr 2015; published 21 Apr 2015

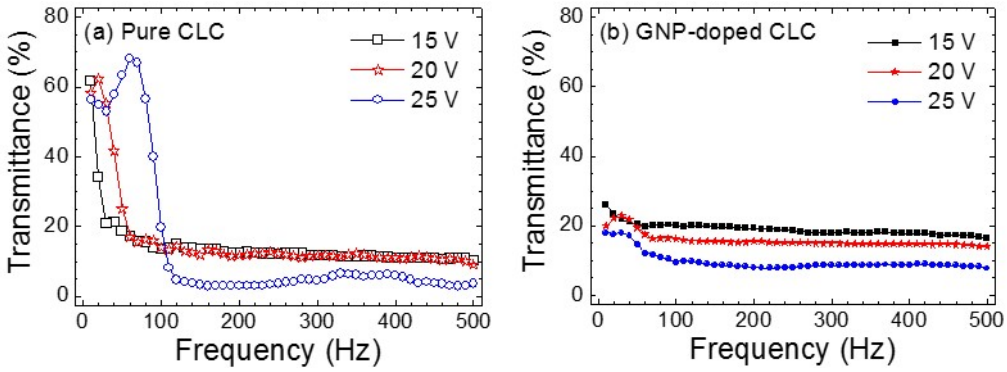

Fig. 7. Frequency-dependent transmittance of the (a) undoped and (b) GNP-doped CLC cells under the application of various voltages.

Furthermore, Fig. 7 shows the frequency-dependent transmittance of the two cells driven by various voltages. Based on the results of Fig. 5, the applied voltages selected are higher than $V_{P–FC}$ of the cells. Starting from f = 500 Hz, in the case of pure CLC, the transmission for three voltage conditions gets higher as the frequency decreases to a critical value owing to the induced FC-to-ULH texture transition, as shown in Fig. 7(a). It is found that the critical frequency for the induction of the FC-to-ULH texture transition ascends at elevated voltages. This result is in a good agreement with the general picture of hydrodynamic instabilities in nematic LCs, in which the required voltage for the onset of EHD effect is proportional to $f^{1/2}$ [38]. In contrast, as revealed in Fig. 7(b), the transmission of the GNP-doped CLC cell under each voltage condition is nearly invariant with respect to the frequency, indicating the stability of the FC state in the given frequency region (i.e., f = 10–500 Hz) and thus confirming again the suppression of the FC-to-ULH texture transition.

4. Conclusions

The ionic behavior and electro-optical responses of the CLC doped with GNPs have been investigated by a set of experimental methods, including temperature-dependent dielectric spectroscopy, microscopic observations of optical textures, and measurements of voltage- and frequency-dependent transmittance as well as transmission spectra. Comparison of spectral properties between GNP-doped and pure CLC cells in the static state (namely, the planar LC texture) indicates that a content of 0.5 wt% of GNPs dispersed in the CLC is not sufficient to modify the helically molecular structure and, hence, the profile of the reflection band. Data of dielectric tan δ spectra in the frequency range 1–1000 Hz, where the change in complex permittivity as a function of the frequency is characterized primarily by the behavior of ionic migration, show that the values of both tan δ maximum and f_R at a given temperature in the GNP-doped CLC cell are lower than those in the pure CLC counterpart. As the sum of the charge and discharge times of ions (i.e., the relaxation time) is inversely proportional to f_R, this suggests the ion-trapping effects of GNPs. The obtained $\varepsilon'(f)$ and $\varepsilon''(f)$ data show that the GNPs as efficient ion-suppressers at 0.5 wt% in the CLC reduce the ion density by approximately 32% and diminish the diffusivity by the enhanced LC viscosity. Under voltage application to the GNP-doped cell, the threshold voltage for the P-to-FC texture transition is remarkably reduced from 11 to 6 V, presumably due to the presence of GNPs as topological defects. The dispersed GNPs can serve as nuclei creating significant spatial variations in molecular ordering. When the CLC texture is transformed from P to FC state, the conservation of the FC state in the GNP-doped CLC cell under applied voltage is nearly frequency-independent whereas an additional FC-to-ULH texture transition, caused by the EHD effect, is generated in the pure CLC cell at lower frequencies. The absence of low-frequency FC-to-ULH texture transition in the GNP-doped cell arises from the suppression of the ionic effect and, in turn, the EHD effect.

#234759 - $15.00 USD Received 17 Feb 2015; revised 16 Apr 2015; accepted 16 Apr 2015; published 21 Apr 2015

Acknowledgments

This work was financially supported by the Ministry of Science and Technology, Taiwan, through grant Nos. 103-2923-M-009-003-MY3 and 103-2811-M-009-077.

#234759 - $15.00 USD Received 17 Feb 2015; revised 16 Apr 2015; accepted 16 Apr 2015; published 21 Apr 2015